Registry No. Cu, 7440-50-8; hydrogen ion, 12408-02-5; cytochrome *c* oxidase, 9001-16-5.

References

Apell, H.-J., & Läuger, P. (1986) *Biochim. Biophys. Acta 861*, 302.

Babcock, G. T., & Callahan, P. M. (1983) *Biochemistry 22*, 2314.

Benesch, R., & Benesch, R. E. (1962) *Methods Biochem. Anal. 10*, 43.

Blair, D. F., Bocian, D. F., Babcock, G. T., & Chan, S. I. (1982) *Biochemistry 21*, 6928.

Blair, D. F., Witt, S. N., & Chan, S. I. (1985) *J. Am. Chem. Soc. 107*, 7389.

Blair, D. F., Gelles, J., & Chan, S. I. (1986) *Biophys. J. 50*, 713.

Boyer, P. D. (1954) *J. Am. Chem. Soc. 76*, 149.

Buse, G., Meinecke, L., & Bruch, B. (1985) *J. Inorg. Biochem. 23*, 149.

Casey, R. P. (1986) *Methods Enzymol. 126*, 13.

Casey, R. P., Chappel, J. B., & Azzi, A. (1979a) *Biochem. J. 182*, 149.

Casey, R. P., Thelen, M., & Azzi, A. (1979b) *Biochem. Biophys. Res. Commun. 87*, 1044.

Casey, R. P., O'Shea, P. S., Chappell, J. B., & Azzi, A. (1984) *Biochim. Biophys. Acta 765*, 30.

Darley-Usmar, V. M., Capaldi, R. A., & Wilson, M. T. (1981) *Biochem. Biophys. Res. Commun. 103*, 1223.

DeVault, D. (1971) *Biochim. Biophys. Acta 225*, 193.

Finel, M., & Wikström, M. (1986) *Biochim. Biophys. Acta 851*, 99.

Gelles, J., & Chan, S. I. (1985) *Biochemistry 24*, 3963.

Gelles, J., Blair, D. F., & Chan, S. I. (1986) *Biochim. Biophys. Acta 853*, 205.

Hartzell, C. R., & Beinert, H. (1974) *Biochim. Biophys. Acta 368*, 318.

Hill, B. C., & Greenwood, C. (1984) *FEBS Lett. 166*, 362.

Hill, B. C., & Robinson, N. (1986) *J. Biol. Chem. 261*, 15356.

Kagawa, Y., & Racker, E. (1971) *J. Biol. Chem. 246*, 5477.

Konstantinov, A., Vygodina, T., & Andreev, I. M. (1986) *FEBS Lett. 202*, 229.

Li, P. M., Gelles, J., Chan, S. I., Sullivan, R. J., & Scott, R. A. (1987) *Biochemistry 26*, 2091.

Luthe, D. S. (1983) *Anal. Biochem. 135*, 230.

Malmström, B. G. (1982) *Annu. Rev. Biochem. 51*, 21.

Müller, M., Thelen, M., O'Shea, P., & Azzi, A. (1986) *Methods Enzymol. 126*, 78.

Naqui, A., Chance, B., & Cadenas, E. (1986) *Annu. Rev. Biochem. 55*, 137.

Püttner, I., Carafoli, E., & Malatesta, F. (1985) *J. Biol. Chem. 260*, 3719.

Sone, N., & Nicholls, P. (1984) *Biochemistry 23*, 6550.

Tanford, C. (1983) *Annu. Rev. Biochem. 52*, 379.

Thelen, M., O'Shea, P. S., Petrone, G., & Azzi, A. (1984) *J. Biol. Chem. 260*, 3626.

Tzudzuki, T., Orii, Y., & Okunoki, K. (1967) *J. Biochem. (Tokyo) 62*, 37.

Wikström, M. K. F. (1977) *Nature (London) 266*, 271.

Wikström, M., & Casey, R. P. (1985) *J. Inorg. Biochem. 23*, 327.

Wikström, M., Krab, K., & Saraste, M. (1981) *Cytochrome Oxidase—A Synthesis*, Academic Press, London.

Intermediates in the Refolding of Ribonuclease at Subzero Temperatures. 1. Monitoring by Nitrotyrosine Absorbance†

Roger G. Biringer‡ and Anthony L. Fink*

Department of Chemistry, The University of California, Santa Cruz, California 95064

Received September 29, 1986; Revised Manuscript Received July 13, 1987

ABSTRACT: Derivatives of ribonuclease A in which tyrosines-73, -76, and -115 were nitrated have been synthesized, purified to homogeneity, and characterized by NMR, isoelectric points, absorbance spectra, and catalytic activity. The positions of their reversible thermal unfolding transitions were determined in 35% methanol at pH* 3.0 and 6.0. In the present study the kinetics of the refolding of these nitrotyrosine derivatives were measured at −15 °C at pH* 3.0 and 6.0 by using a cryosolvent composed of 35% aqueous methanol. The rates of folding of different regions of the molecule were determined by using the nitrotyrosines as environmentally sensitive probes. Multiphasic kinetics were observed for the refolding of the nitro-Tyr-115, -73, and -76 derivatives. The native environment about Tyr-115 was formed more rapidly than that about Tyr-73 and -76, and the native environment about both these tyrosines was attained much sooner than the native state itself, as judged by other probes. The results indicate that different regions of the molecule attain their native environments at different rates. This observation shows that the folding pathway must involve partially folded intermediate states.

The process whereby a polypeptide chain folds into its native conformation is of major biological importance. Current interest in the mechanisms and pathway of protein folding centers on the nature of intermediate states. Difficulties exist in detecting intermediates during protein folding due to their low concentrations and short lifetimes. Preliminary results have indicated that the use of low temperatures and aqueous–organic cryosolvents may be very useful in permitting the stabilization of partially folded intermediates (Biringer & Fink,

† This research was supported by a grant from the National Science Foundation.

‡ Present address: Department of Chemistry, San Jose State University, San Jose, CA 95192.

0006-2960/88/0427-0301$01.50/0

1982a,b; Fink & Painter, 1987).

Previous studies have shown that RNase A[1] is stable and functional in methanol cryosolvents, at temperatures below the thermal denaturation transition (Fink & Painter, 1987; Fink et al., 1987), and proton NMR and crystallographic results indicate that the conformation of the *native* state is similar in aqueous–methanol cryosolvents and in aqueous solution (Biringer & Fink, 1982a,b; Campbell & Petsko, 1987).

If the early stages of folding involve predominantly secondary structure, then low temperatures, which strengthen H bonds, would be expected to stabilize such early intermediate states. If the later stages of folding involve the packing together of regions of secondary structure, predominantly through hydrophobic interactions, these would be expected to be weakened at lower temperatures. Thus low temperatures should increase the discrimination between the stability of early and late folding intermediates, thus making the former more readily detectable. The effects of increasing organic cosolvent on the folding process are attributed predominantly to the increased hydrophobicity of the solvent. Thus for the above-mentioned model of folding in cryosolvent, both the unfolded and partially folded states (with their exposed nonpolar residues) will be stabilized relative to N. Hence, the net effect of folding in cryosolvents at subzero temperatures will be to stabilize the partially folded intermediates relative to the native state.

Regarding the relevance of the folding pathway in aqueous methanol to that under physiological conditions, we believe that such studies provide a *model* for the process in aqueous solution. Although the potential energy surface for folding will differ in the presence of methanol, and as a function of temperature, there is no reason at present to believe that the determinants guiding the folding at subzero temperatures in cryosolvent will not be the same as at higher temperatures in aqueous solution.

One approach to obtaining information about intermediates in protein folding is to use a series of probes located throughout the structure of the molecule which, minimally, can signal whether their environment corresponds to that of the solvent-exposed, unfolded state or the native, folded state. Thus by monitoring the time-dependent changes in the probe as folding occurs, one can determine at which stage that particular region of the molecule attains its native environment.

The refolding of RNase is complicated by the existence of fast- and slow-refolding forms, attributed to different unfolded states, due, at least in part, to proline cis/trans isomerization. At least two different intermediates have been identified on the pathway of the major slow-refolding species, an early intermediate detected on the basis of H/D exchange trapping experiments (Nall et al., 1978; Schmid & Baldwin, 1979; Kim & Baldwin, 1980) and a native-like, late intermediate (Cook et al., 1979; Schmid, 1981, 1983; Schmid & Blashek, 1981; Mui et al., 1985).

In the present paper we examine the kinetics of folding of RNase in which three of the six tyrosine residues have been selectively nitrated to provide chromophoric probes of the regions about Tyr-73, -76, and -115. These may be correlated with other probes, such as histidine NMR (Biringer & Fink, 1982b), tyrosine fluorescence and absorbance (Biringer & Fink, 1988), the binding of a competitive inhibitor and the return of catalytic activity (Biringer et al., 1988), and double-jump assays to monitor intermediate accumulation (Biringer & Fink, 1988). In future papers we will report on the results with other probes. The synthesis and characterization (including the position of the thermal unfolding transition) of these very useful derivatives are given in detail since they have not been reported previously.

Experimental Procedures

Purification of RNase A. Chromatographically "pure" ribonuclease A was purchased from Calbiochem-Behring Corp. The enzyme was further purified on a Sephadex SPC-25 ion-exchange column (1.5 × 25 cm, 0.13 M phosphate, pH 6.5). In a typical purification, a 200-mg sample was applied to the column in 1–2 mL of the eluting buffer. This procedure facilitates the separation of RNase S and aggregated material from RNase A. The protein fraction was desalted by ultrafiltration on an Amicon ultrafiltration assembly with a PM-10 membrane. The solution taken directly from the column was concentrated to 1–2 mL and then diluted to 50 mL with deionized distilled water. This desalting procedure was repeated 3–4 times. Analysis of the desalted material revealed that the phosphate concentration was no more than 0.24 mol %. The purified material was homogeneous by analytical IEF and was lyophilized and stored at −20 °C.

Materials. Ultrapure guanidine hydrochloride was obtained from Research Plus Corp.; *N*-acetyltyrosine ethyl ester was obtained from Sigma Chemical Co. Spectrograde methanol was obtained from Mallinckrodt. Tetranitromethane was purchased from Aldrich, and isoelectric focusing ampholytes were from LKB or Brinkmann. All cryosolvents were mixed on a volume/volume basis. Either sodium acetate (pH* 6.0) or sodium formate (pH* 3.0) buffers were used at a concentration of 0.033 M. The presence of the methanol causes a substantial increase in the pK of the ionizing groups of these weak acids; hence acetate is still in its buffering range at pH* 6.0. All buffer solutions were filtered prior to use with a 0.5-μm Teflon filter (Millipore Corp.) in a syringe-type filtering apparatus. Protein solutions were filtered through a 0.2-μm cellulose filter in a centrifuge-mounted device (Bioanalytical Systems Inc.). It should be noted that disposable syringes must be meticulously washed prior to use, as the plunger lubricant is easily extracted into both aqueous solvents and cryosolvents. The lubricant compounds absorb strongly in the UV and near-UV, and the absorbance has a strong temperature dependence (Petersen, 1981).

Preparation of $C^{\epsilon 115\text{-}NO_2}$-RNase, $C^{\epsilon 115,76\text{-}NO_2}$-RNase, and $C^{\epsilon 115,76,73\text{-}NO_2}$-RNase. The nitration of solvent-exposed tyrosines was accomplished by reaction of RNase A with tetranitromethane. In a typical preparation a 25-mg sample of protein was dissolved in 10 mL of 0.13 M tris(hydroxymethyl)-aminomethane (Tris) at pH 8.0. A thirty- or sixtyfold molar excess of tetranitromethane was then added as a 10% (w/v) solution in 90% (v/v) methanol. The former concentration produces predominantly singly and doubly nitrated derivatives while the latter favors the doubly and triply nitrated derivatives (see below). The reaction was allowed to proceed for 20 min at room temperature with constant stirring and then was quenched by passing the solution through a Sephadex G-25 column (2.5 × 6 cm) and eluting with 0.1 M ammonium hydroxide. This procedure produces base line separation of residual tetranitromethane and nitroformate (the major byproduct) from the protein fraction. The process was generally repeated with three additional 25-mg samples, and the protein fractions were combined prior to further purification. The

[1] Abbreviations: RNase, ribonuclease A; IEF, isoelectric focusing; pH*, apparent pH or protonic activity of aqueous–methanol cryosolvent; *nitro-Tyr-115 or* $C^{\epsilon 115\text{-}NO_2}$-RNase, derivative of RNase A in which Tyr-115 has been nitrated at the ϵ-position; Gdn·HCl, guanidine hydrochloride; 2′,3′-CMP, cytidine 2′,3′-cyclic monophosphate; N, native state; U, unfolded state.

protein solution was acidified to pH 4 in order to improve the solubility and ultrafiltered 4–5 times with a fiftyfold excess of deionized water in an Amicon filtration assembly fitted with a PM-10 membrane. The filtration step is necessary in order to remove ammonia and residual nitroformate, which binds rather tightly to the protein. The final solution was frozen, lyophilized, and stored at −20 °C until further use.

The reaction of tetranitromethane with proteins also results in the production of covalently cross-linked dimers (Williams & Lowe, 1971; Vincent et al., 1970). The dimeric material was removed chromatographically as follows. The lyophilized powder was dissolved in 1–2 mL of 0.13 M phosphate, pH 6.5, loaded on a Sephadex SPC-25 (1.5 × 45 cm) or a G-75 column (2.5 × 20 cm), and eluted with the same buffer. The monomeric fraction was then ultrafiltered as above, frozen, and lyophilized.

At this point in the preparation the lyophilized powder consists of a mixture of various nitrated RNases and unmodified RNase. Fractionation into individual components was accomplished with preparative isoelectric focusing. A glass plate (10 × 20 cm) was coated with a 0.3-cm layer of a 6.4% (w/v) gel suspension containing Sephadex IEF resin and 2.4% (w/v) carrier ampholytes, pH 8–9.5. Lyophilized protein from two preparations (70–80 mg) was dissolved in a minimum of carrier ampholytes [2.4% (w/v), pH 8–9.5] and mixed with a small amount of gel suspension. The mixture was then applied to a 1 × 8 cm trough cut in the center of the gel bed. Voltage was applied with platinum wires inserted through filter paper tubes which had been soaked in electrolyte. The anode electrolyte was 1% (w/v) solution of pH 6–8 ampholytes (Brinkmann), and the cathode electrolyte was 0.1 M NaOH. Focusing was performed for 16–18 h at 8 °C with an applied potential of 300 V. This was followed by an additional 4 h with an applied potential of 800–1000 V.

The yellow-colored bands were individually removed from the plate and placed in sintered glass filtering funnels. The gel beads were washed until they no longer appeared yellow in color. The volume of the eluant was reduced, and the ampholytes were removed by ultrafiltration. The protein fraction was then frozen and lyophilized.

Each of the protein fractions was purified a second time by isoelectric focusing by the above procedure, with the following changes: (1) a 5 × 20 cm plate was used; (2) the protein was applied as a concentrated solution in 2.4% (w/v) carrier ampholytes, pH 8–9.5. For analytical isoelectric focusing we used preformed acrylamide plates (pH 3–10, Serva Corp.). Anode and cathode buffers were prepackaged solutions obtained from Serva. Protein solutions were applied to the gel plates with protein concentration in the 2–5 mg/mL range. Focusing was performed at 8 °C and 3.5-W constant power for 2 h or incremented from 200 to 1000 V over a 2-h period. Plates were fixed with 20% trichloroacetic acid (w/v) and stained with Coomassie blue. Marker proteins were obtained from FMC Corp.

Reversible Thermal Unfolding. The reversible unfolding/refolding of the nitrated derivatives of RNase in 35% methanol was monitored at pH* 3.0 and 6.0 by absorbance change at 300 nm. Typical concentrations for RNase were varied between 14 and 31 μM for both pH* values. All solution volumes were 3.0 mL. The matched reference cell was filled with an aliquot of the buffer used to dissolve the protein in order to minimize the thermally dependent signal generated by the solvent. Temperature control was provided by a Neslab RTE-8 bath. The cell compartment was constantly purged with dry gas. The temperature was varied as a linear ramp at 0.3 °C/min with a temperature bath programmer (Neslab Corp.), and the process was reversed at the same rate. The temperature was maintained at the end of the ramp for a minimum of 20 min before reversal was initiated. In many of the experiments the procedure was subsequently repeated a second time with the same sample.

In order to ensure that the rate at which the temperature was changed allowed equilibrium to be established between the unfolded states of the protein, the temperature ramp was disengaged at several temperatures and the absorbance monitored as a function of time. This operation was performed at least once for both increasing and decreasing temperature. In all cases the absorbance remained unchanged for the time (10–20 min) the temperature was held constant. The absence of change indicates that equilibrium was established along the temperature ramp in all cases.

The midpoints of the unfolding/refolding transitions were calculated by first extrapolating the linear regions of the low- and high-temperature portions of the curves across the transition zone. The fraction of the protein in the unfolded state (f_u) was then calculated by the relation:

$$f_u = U/(U + N)$$

where U is the difference between the absorbance at a particular temperature and the high-temperature extrapolation and N is the difference between the absorbance and the low-temperature extrapolation at the same temperature (see Figure 4).

Control experiments were performed to establish that the protein concentrations utilized in these experiments did not result in aggregation. The following observations and experiments demonstrate that aggregation did not occur. (1) The thermal unfolding/refolding experiments were performed over a range of concentrations. In all cases, the shape of the curve and T_m were identical. If aggregation were to accompany the transition, both the shape and T_m would show concentration dependence. (2) Aggregation, when observed, is unidirectional (i.e., irreversible) rather than being an equilibrium process. Control experiments were performed in which the temperature ramp was disengaged and the absorbance signal monitored as a function of time. In all such tests, the absorbance remained steady for the duration of the experiment (20 min). If the protein were aggregating, the absorbance would change as a function of time. (3) The NMR spectra of the nitrated derivatives show sharp resonances for all protons at all temperatures. If the protein were aggregating, broad resonances would result. The concentrations used in the NMR experiments are many times higher than those used in the thermal unfolding experiments.

Unfolding in Guanidine Hydrochloride. In a typical experiment the absorbance of the native protein was determined by injecting an aliquot (50 μL) of a stock solution (0.75 mM protein, 35% methanol, pH* 3.0, 0.033 M sodium formate, 25 °C) into 1.0 mL of 35% methanol buffered at pH* 3.0 or 6.0 at −15 °C. The absorbance of the unfolded protein was determined similarly except that the 1.0 mL of buffer was also 5.0 M in guanidine hydrochloride. The dilution effect on the signal produced by the guanidine was calculated by injecting a 50-μL aliquot of the stock buffer without enzyme into 1.0 mL of the 5 M guanidine buffer. The effect of guanidine on the signal produced by solvent-exposed nitrotyrosines was determined by injecting a 50-μL aliquot of 4.5 mM *N*-acetylnitrotyrosine ethyl ester into 1.0 mL of the guanidine-containing buffer. In each case the signals were monitored as a function of time until the value remained constant. The appropriate combination of these measurements was used to

calculate the absorbance difference between native and unfolded RNase A.

Experiments to Detect Deamidation. The nitrated ribonuclease derivatives were tested for the presence of thermally induced deamidation under each set of conditions employed in the thermal denaturation studies. An aliquot was taken from the sample solution after completion of the unfolding/refolding transition and stored at −20 °C. A sample was applied to an analytical isoelectric focusing gel (pH 3–10) (Servalyte Corp.) along with samples that had not been heated as reference standards. The plate was focused at 4-W constant power for 4 h and then stained with Coomassie blue.

Refolding Kinetics. The refolding of $C^{\epsilon 115\text{-}NO_2}$-RNase A, $C^{\epsilon 115,76\text{-}NO_2}$-RNase A, and $C^{\epsilon 73,76,115\text{-}NO_2}$-RNase A was examined by following the decrease in absorbance at 300 nm. At this and higher wavelengths there are negligible changes in absorbance in unmodified RNase A during folding, and folding at lower wavelengths is observed as an *increase* in absorbance.

In a typical refolding experiment, an aliquot of concentrated protein solution was taken up into a gas-tight microsyringe (Hamilton) and incubated for 10 min at 70 °C in a water bath. Previous experiments using NMR had demonstrated that these conditions result in the apparent complete unfolding of RNase (Biringer & Fink, 1982a). In addition, this temperature is above the thermal denaturation transition as measured by absorbance change for the nitrotyrosine derivatives (see Results and Discussion). In some experiments the protein was unfolded in 5 M Gdn·HCl, pH 2.0, 25 °C, for 30 min. The syringe contents were then injected into a thermostated cuvette containing 1.0 mL of cryosolvent held at −15 ± 0.2 °C. Immediately after injection the solution was mixed with a *precooled*, vibrating plumper (Calbiochem) for 20 s. The time-dependent changes in the absorbance or fluorescence were directly accumulated on a microcomputer interfaced to the spectrophotometer or taken directly from the chart paper. Experiments were terminated after no further change in the absorbance was observed for at least 1000–2000 s.

Control experiments to compare the rate of refolding of the nitrated derivatives to that of the unmodified protein were carried out as follows. The refolding was monitored by changes in absorbance at 286 nm for comparison with corresponding data for the unmodified enzyme (Biringer & Fink, 1988). Otherwise, the experimental procedures were the same as those used in monitoring the nitrotyrosines at 300 nm. The large amplitude changes due to the nitrotyrosine group prevented observation of the faster transients detected in the unmodified enzyme.

Protein stock solutions were 0.35–0.75 mM, pH* 3.0, in 0.033M sodium formate in 35% methanol. In the pH* 3.0 experiments 50- or 60-μL aliquots were injected into 1.0 mL of the pH* 3.0 buffer. In the pH* 6.0 experiments 60-μL aliquots of the pH* 3.0 stock solution were injected into 1.0 mL of sodium acetate buffer adjusted to pH* 6.2 to give a final pH* of 6.0. In some cases smaller aliquots of stock solution were used.

Kinetic Data Analysis. Data from all experiments were analyzed by a curve-fitting program, REDUCE, based on a linear expansion least-squares algorithm described by Bevington (1969) and written by Dr. S. Koerber.

The multiphasic kinetics were analyzed by the curve-fit routine in a stepwise fashion. In each case, the slowest observed phase was analyzed as a single exponential. The best fit data were then subtracted from the entire data set. The entire process was then repeated on the resulting data set. The "stripping" procedure was repeated until only a single exponential remained. Accurate kinetic parameters could be obtained for multiphasic data as long as the rate constants differ by a factor of ≥3. In nearly all cases the measured transients differed by a factor of about 10 in rate. Kinetic analyses were also carried out by using a curve-fitting procedure for multiple parallel exponential processes, as well as graphically by means of a least mean squares fit procedure. The graphical method was used primarily for calculation of starting parameters for the fitting routine and as a check on the accuracy of the fitting procedure. Similar results were obtained with all three methods.

Refolding kinetics data for $C^{\epsilon 76\text{-}NO_2}$-RNase were obtained by subtraction of the absorbance data from an average of three experiments with the $C^{\epsilon 115\text{-}NO_2}$-RNase derivative from that of several $C^{\epsilon 115,76\text{-}NO_2}$-RNase experiments. The amplitudes were converted to percent of the total expected amplitude change. Similarly, for nitro-Tyr-73 the refolding kinetics were obtained by subtracting the averaged data of six experiments with the dinitro derivative from those of the trinitro derivative.

Amplitude Calculations. The amplitudes of each folding phase are presented as a percentage of the amplitude obtained from the difference between native and unfolded protein. This was obtained by comparison of the absorbance at 300 nm of the native and unfolded nitrated derivatives measured at −15 °C, in 35% methanol at pH* 3.0 and 6.0. The unfolded protein was obtained by making the cryosolvent 5 M in Gdn·HCl.

Control Experiments for Refolding Kinetics Measurements. A number of potential problems may arise when experiments are performed in nonaqueous systems and at low temperatures. Since the protein solubility decreases inversely with both cryosolvent concentration and temperature, the observed signals could be due to aggregation. Mixing artifacts can also produce signals in the early portion of any kinetic experiment.

Both aggregation and folding can result in the burial of exposed tyrosine moieties and therefore produce similar signals. A number of experiments were conducted in order to test for the presence of aggregation. High concentrations of protein were examined by light scattering and gel permeation chromatography and proved negative for the presence of aggregates in unmodified ribonuclease (Biringer & Fink, 1982a,b).

Rayleigh light scattering experiments were performed with a fluorometer in which both the excitation and emission were set to 300 nm, and the folding reaction was monitored. The chosen conditions were those most likely to produce aggregation, pH* 6.0 and 50% methanol. A series of unmodified protein concentrations were utilized in order to determine the minimum concentration necessary to produce anything that resembled aggregation. The study showed that minor increases in the scattering could be produced only with final protein concentrations above 36 μM. The presence of aggregates was not proven, however. The concentrations used in the folding experiments discussed above were considerably lower. Second, the refolding kinetics were measured in 35% methanol in which the protein exhibits superior solubility compared to higher methanol concentrations. The data indicate that aggregation does not occur under the experimental conditions used.

Light scattering experiments were performed for the folding reaction of the nitrated derivatives in the same fashion as noted above, with the exception that the experimental conditions were those used in the absorbance-monitored experiments. The reaction was followed for the duration of the folding reaction. In all cases there was no change in the signal, indicating no light scattering process and hence no detectable aggregation during the refolding of the nitrated derivatives.

The addition of hot solvents to cold solutions induces transitory thermal gradients. The experimental procedure used results in the production of such gradients which are observed as an initial fluctuation in the apparent absorbance of the sample. It is presumably an index of refraction effect. In order to determine the time course of this event, the thermal perturbation time was measured under each set of conditions and for each monitoring technique. The time course was measured as follows.

The refolding kinetics experiments were modeled by the injection of hot solvent (70 °C, 35% methanol, pH* 3.0) into cold buffer in the presence and absence of native protein. The solvent volumes and composition were identical with those used in the folding experiments. In the cases where enzyme was present, the concentrations were the same as those used in the folding experiments. The signal was monitored at the wavelengths used for the particular protein until the signal was flat for at least 10 min. All perturbations monitored by absorbance ceased well within 60 s after the hot solvent was introduced. By 30 s the amplitude of the thermal mixing artifact was ≤10% of the signal observed at that time in the refolding experiments. The thermal artifact produces a decrease in the apparent absorbance. The maximum temperature measured in the sample cell on addition of the largest aliquot of the hot solution was −11 °C. Thus, although the use of thermally unfolded protein leads to the potential for some refolding to occur during the cooling/mixing process, given the rates of the slow-refolding reactions, it is reasonable to assume that no significant refolding of the slow-refolding species would occur during the time period for mixing. This was confirmed in the double-jump unfolding assays (Fink & Biringer, 1987) which showed only 20% native protein present at the earliest times of refolding (arising from the 20% fast-refolding state).

Because of potential limitations associated with the use of thermally unfolded protein samples in the refolding experiments we also ran some experiments where the sample was unfolded with Gdn·HCl. The protein was unfolded at 25 °C in aqueous Gdn·HCl (5 M) at pH 2.0 (glycine buffer) for 30 min. The solution was then cooled to 0 °C and a 50-μL aliquot added to 1.0 mL of 35% methanol at −15 °C to give final values of pH* 3.0 or 6.0 and 0.24 M Gdn·HCl. The refolding kinetics were monitored as noted above for the dinitrotyrosine derivative, and also by fluorescence for unmodified protein (Biringer & Fink, 1988). The addition of an aliquot of 5 M Gdn·HCl in aqueous methanol solution to cryosolvent at subzero temperatures leads to substantial spectral perturbations during mixing, and hence longer mixing times are necessary, whether or not protein is present. Consequently, the refolding reaction could not be monitored at early times.

Similar transients were observed, however, whether the protein was unfolded in Gdn·HCl or thermally. For example, for unmodified RNase the rate constants for the two phases observed with fluorescence emission at pH* 3 or 6 were essentially identical for both methods of unfolding, and the total amplitude change observed was slightly larger for the Gdn·HCl-unfolded system (31% vs 24% for thermal unfolding). Similarly, the rate constants for the two phases observed in the refolding of 76,115-dinitrotyrosyl-RNase (pH* 3) were the same within experimental error (Table V). However, due to the spectral perturbations in the early stages of the reaction it was not possible to accurately measure the amplitude of the first phase.

Results and Discussion

Preparation of $C^{\epsilon 115\text{-}NO_2}$-RNase, $C^{\epsilon 115,76\text{-}NO_2}$-RNase, and $C^{\epsilon 115,76,73\text{-}NO_2}$-RNase. Nitration with tetranitromethane was first employed for modification of RNase A by Beaven and Gratzer (1968) and later by Seagle and Cowgill (1976). In each of these studies it was found that exhaustive nitration, under conditions that favored the native state of RNase A, produced a maximum of three nitrated tyrosines. Subsequently, Van Der Zee et al. (1977) showed that the tyrosyl residues exhibited a differential reactivity toward nitration in the order Tyr-115 > -76 > -73.

Experimentation with the nitration conditions indicated that a thirtyfold molar excess and a reaction time of 20 min maximizes the yield of singly and doubly nitrated derivatives. A sixtyfold excess and 20-min reaction time maximizes the yield of doubly and triply nitrated derivatives. Various other modifications to the reported methods were necessary to produce homogeneous material.

The production of covalently cross-linked protein with tetranitromethane is the major limitation of this methodology (Williams & Lowe, 1971). In order to reduce the amount of dimer, the protein concentration must be kept to a minimum. The isoelectric focusing produces three well-separated yellow bands; however, a second focusing was necessary to produce homogeneous product. The overall yields from the preparation utilizing a thirty-fold molar excess of tetranitromethane were, on the average, as follows: singly nitrated = 10%; doubly nitrated = 9%; triply nitrated = 1–2%. The overall yields from the preparation utilizing a sixtyfold molar excess of tetranitromethane were, on the average, as follows: singly nitrated = 1–2%; doubly nitrated = 16%; triply nitrated = 11%.

Characterization of Nitrated Ribonuclease Derivatives by IEF and NMR. The homogeneity of the derivatives was determined by analytical isoelectric focusing and NMR spectra. For each derivative analytical IEF showed a single sharp band, consistent with the proteins being homogeneous in terms of the number of nitrations per molecule. This result does not confirm absolute homogeneity, as it might be possible that an equal number of nitrations at different sites may produce derivatives with similar or identical p*I*'s. The observed isoelectric points for each of the proteins were as follows: RNase A, 9.3; mononitro-RNase, 9.0; dinitro-RNase, 8.7; and trinitro-RNase, 8.0.

The NMR spectra of the aromatic region of each derivative and RNase A in ^2H_2O are given in Figures 1 and 2 for pH* 3.0 and 7.0, respectively. Each nitrated tyrosine produces a sharp singlet for the δ ring proton adjacent to the nitro group. Such resonances are always located downfield of the aromatic envelope. The mononitro derivative shows this singlet near 8.5 ppm at pH* 3.0 and 8.4 ppm at pH* 7.0. The dinitro derivative shows the same resonance and, in addition, one other near 8.2 ppm at pH* 3.0 (under His-48 C-2H) and 8.0 ppm at pH* 7.0. The trinitro derivative shows the same singlets as the dinitro plus an additional one near 7.8 ppm at pH* 3.0 and 7.6 ppm at pH* 7.0. The fact that each of the three peaks differs so widely in chemical shift indicates that each resonance is peculiar to a particular nitration site. Since each derivative also exhibits the expected number of such resonances, each must be homogeneous with respect to the nitration sites. In addition, the fact that the derivatives share common resonances confirms the previous report that the nitration of tyrosines in RNase A is a sequential process. The NMR spectra, Figures 1 and 2, also confirm the assignment of the nitrated tyrosine residues, based on the Tyr assignments of Lenstra et al. (1979).

Properties of Nitrated Ribonuclease. The absorbance spectra for $C^{\epsilon 115\text{-}NO_2}$-RNase, $C^{\epsilon 115,76\text{-}NO_2}$-RNase, and $C^{\epsilon 115,76,73\text{-}NO_2}$-RNase are given in Figure 3. The absorbance spectrum for *N*-acetyl-ε-nitrotyrosine is included for com-

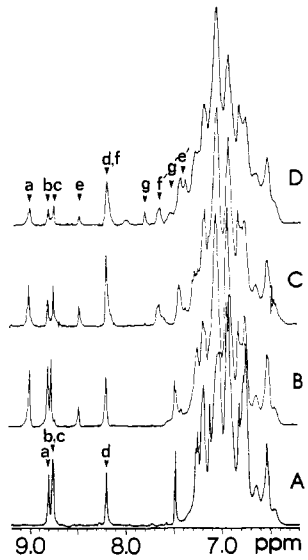

FIGURE 1: NMR spectra of the aromatic region of RNase and chemically modified derivatives in ^2H_2O, pH* 3.0, and 0.1 M KCl and at 22 °C: (A) RNase A; (B) $C^{\epsilon 115\text{-}NO_2}$-RNase; (C) $C^{\epsilon 115,76\text{-}NO_2}$-RNase; (D) $C^{\epsilon 115,76,73\text{-}NO_2}$-RNase. The labeled resonances are assigned as follows (Lenstra et al., 1979; Biringer and Fink, unpublished results): a = His-12 C2; b = His-119 C2; c = His-105 C2; d = His-48 C2; e = Tyr-115 δ; e' = Tyr-115 δ'; f = Tyr-76 δ; f' = Tyr-76 δ; g = Tyr-73 δ; f' = Tyr-73 δ'. In the unmodified protein the resonances from His-105 and -119 overlap due to a combination of the pH and ionic strength.

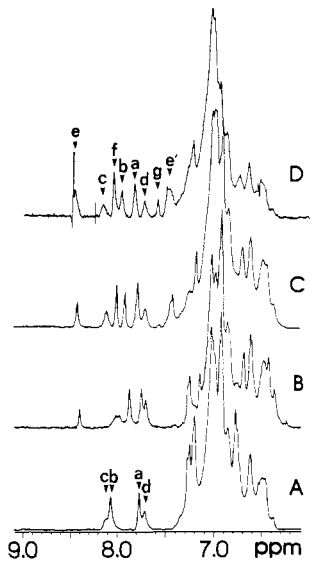

FIGURE 2: NMR spectra of the aromatic region of RNase and chemically modified derivatives in ^2H_2O, pH* 7.0, and 0.1 M KCl and at 22 °C: (A) RNase A; (B) $C^{\epsilon 115\text{-}NO_2}$ RNase; (C) $C^{\epsilon 115,76\text{-}NO_2}$ RNase; (D) $C^{\epsilon 115,76,73\text{-}NO_2}$ RNase. The assignments are given in the legend to Figure 1.

parison. The spectra at pH 3.0 and 8.5 are shown, corresponding to the two ionization states, since the pK of nitro-Tyr in aqueous solution is 6.8 (Garel & Baldwin, 1975).

One feature that each set of spectra has in common is the isosbestic point near 380 nm. The isosbestic points for N-acetyl-ϵ-nitrotyrosine, $C^{\epsilon 115\text{-}NO_2}$-RNase, and $C^{\epsilon 115,76\text{-}NO_2}$-RNase are located at 381 nm. Van Der Zee et al. (1977) reported that the molar absorbance at this wavelength (2200 OD/M nitrotyrosine) can be used to quantitate the extent of tyrosine nitration in nitrated RNase A. Although the methodology is more precise than that of Goto et al. (1971) and Beaven and Gratzer (1968), the present study indicates that it only yields precise values in the case of $C^{\epsilon 115\text{-}NO_2}$-RNase. Application to

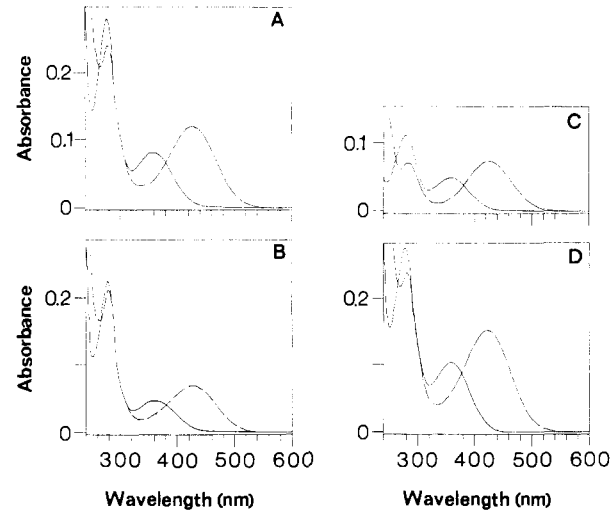

FIGURE 3: Absorbance spectra of chemically modified RNases. Solid lines represent spectra taken at pH 3.0 in 0.1 M sodium formate. The dot–dash lines represent spectra taken at pH 8.5 (ionized nitro-Tyr) in 0.1 M Tris. All concentrations were 18 μM. (A) N-acetyl-ϵ-tyrosine; (B) $C^{\epsilon 115,76,73\text{-}NO_2}$-RNase; (C) $C^{\epsilon 115,76\text{-}NO_2}$-RNase; (D) $C^{\epsilon 115\text{-}NO_2}$-RNase.

Table I: Catalytic Activity of Nitrated Ribonucleases

derivative	act.[a]	derivative	act.[a]
$C^{\epsilon 115\text{-}NO_2}$-RNase	100	$C^{\epsilon 115,76,73\text{-}NO_2}$-RNase	74
$C^{\epsilon 115,76\text{-}NO_2}$-RNase	98		

[a] Activity (act.) is expressed as a percentage of the catalytic activity exhibited by an equal molar amount of unmodified RNase A toward the same substrate, cytidine 2',3'-cyclic monophosphate, under the same experimental conditions (see text).

$C^{\epsilon 115,76\text{-}NO_2}$-RNase obtained in this study results in an underestimation of nitrotyrosine content by 15%.

In the case of $C^{\epsilon 115,76,73\text{-}NO_2}$-RNase the isosbestic point is found at 378 nm. The molar absorbance at this wavelength is 5300 O.D./M. The shift in the isosbestic point shows that the environment about Tyr-73 differs from that of the other tyrosines. Thus the environment about each tyrosine is unique and each makes a different contribution to the total absorbance at a particular wavelength. The crystallographic structure of RNase indicates that there is a hydrogen bond between the side chains of Tyr-73 and Tyr-115. As noted below, nitration of both of these residues results in a significant perturbation of the expected extinction coefficient of nitro-Tyr-73.

The enzymatic activity of the three derivatives toward 2',3'-CMP is given in Table I. The results show that nitration at tyrosines-115 and -76 has no effect on the activity. These results are not unexpected as the two residues are quite exposed to solvent and are located away from the active site. The nitration at position 73 reduces the activity by 25%, consistent with the position of this residue within the active-site cleft.

Thermal Unfolding of Nitrated RNase in Aqueous Solution and 35% Methanol. Typical thermal denaturation curves for the nitrated derivatives in 35% methanol are shown in Figure 4. In each case the absorbance at 300 nm was monitored as a function of temperature. At this wavelength only nitrotyrosines absorb appreciably.

The unfolding transition was fully reversible, on the basis of both NMR and absorbance measurements, although significant hysteresis was noted in the absorbance experiments. The T_m values obtained for the unfolding were identical with those for the refolding. The average values obtained for each experiment are shown in Table II and represent an average of at least three experiments. Garel and Baldwin (1975)

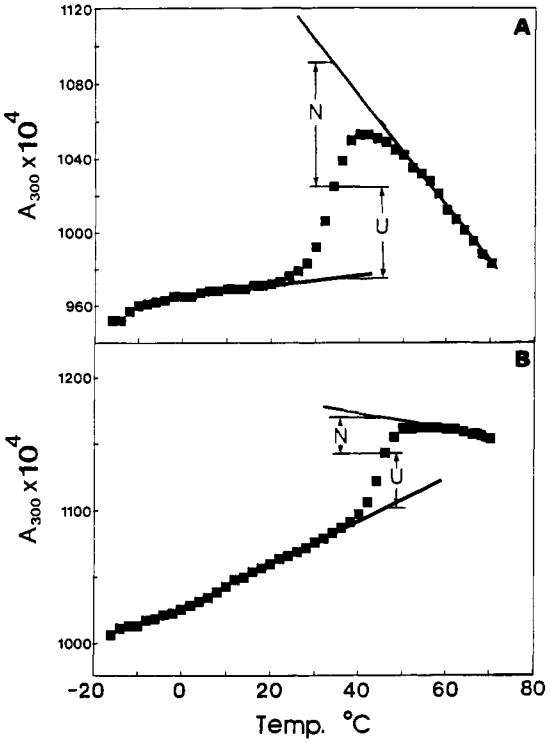

FIGURE 4: Change in absorbance at 300 nm during the first thermal unfolding of nitrated RNase. The fraction of unfolded protein at each temperature was calculated by the method described in the text. (A) $C^{\epsilon 115\text{-}NO_2}$-RNase, pH* 6.0, 35% methanol; (B) $C^{\epsilon 115,76\text{-}NO_2}$-RNase, pH* 6.0, 35% methanol.

Table II: Transition Midpoints for Thermal Denaturation of Ribonuclease and Its Nitrated Derivatives, Determined by Absorbance Changes at 286 or 300 nm

sample	T_m (°C) pH* 3.0	pH* 6.0
35% methanol		
RNase A	38 ± 1	48 ± 0.5
$C^{\epsilon 115\text{-}NO_2}$-RNase	38 ± 2	49 ± 1
$C^{\epsilon 76,115\text{-}NO_2}$-RNase	34 ± 1	44 ± 2
aqueous		
RNase A	44	59

reported that for the trinitro derivative the T_m was depressed from 62 to 61 °C in aqueous solution.

Significant hysteresis of two types was observed in the thermal transition for the nitrated derivatives (Figure 5). Following the first unfolding, the molar absorbance of the *refolded* protein never attained the value initially observed at low temperatures. The difference in molar absorbance was constant for a given derivative under a given set of conditions (pH*). Subsequent unfolding/refolding was reversible to this new absorbance value. Hysteresis was also observed during the transition but is reversible as noted above. In all cases the calculated values of T_m were unaffected by the hysteresis.

The reversible hysteresis could reflect a kinetic event or alternate pathways for the initial unfolding and refolding. In order to examine the former possibility, several experiments were interrupted at different temperatures within the transition region, by disengaging the temperture ramp, and the absorbance was monitored for 20 min at constant temperature. In all cases the absorbance remained constant. Thus the hysteresis is unlikely to be due to a kinetic effect. Consequently, the latter possibility seems more reasonable. The different pathways envisaged would involve only very localized regions of the molecule, especially since the hysteresis did not affect the T_m values.

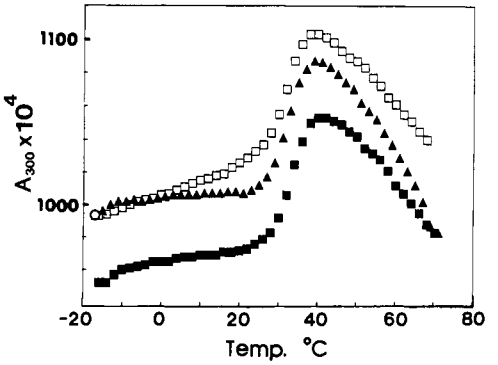

FIGURE 5: Sequential thermal transitions for $C^{\epsilon 115,76\text{-}NO_2}$-RNase at pH* 3.0 in 35% methanol. Monitored by absorbance change at 300 nm. The first unfolding is represented by the filled squares, the first refolding by filled triangles, and the second unfolding by open squares. The circle represents the absorbance after the system was allowed to equilibrate at low temperature following the second unfolding.

Table III: Differences in Molar Extinction Coefficients for Native and Gdn·HCl-Unfolded Ribonuclease and Its Nitrated Derivatives in 35% Methanol at −15 °C[a]

	pH* 3.0	pH* 6.0
RNase A	3000	3260
$C^{\epsilon 115\text{-}NO_2}$-RNase	653	1060
$C^{\epsilon 76,115\text{-}NO_2}$-RNase	1392	1971
$C^{\epsilon 73,76,115\text{-}NO_2}$-RNase	2160	2140
$C^{\epsilon 73\text{-}NO_2}$-RNase[b]	768	169
$C^{\epsilon 76\text{-}NO_2}$-RNase[b]	739	911

[a] The data for RNase A were measured at 286 nm. The values obtained for nitrated ribonuclease were measured by absorbance at 300 nm. The extinction coefficients were obtained from the differences between the absorbance measured in the absence and presence of 5 M Gdn·HCl. [b] By difference.

The irreversible hysteresis is probably due to the nitrated tyrosines attaining a slightly different position in the native protein after the first unfolding. Since the tyrosines were initially nitrated with the protein in the native state, the possible orientations of the side chain were limited and defined by the conformation of the unmodified protein. After nitration, and upon unfolding and subsequent refolding, the nitrotyrosine might prefer a different orientation due to the nitro group and, in this new environment, might have a different molar absorbance. Since the T_m is the same for the initial and subsequent unfolding, there can be no significant effect on the conformation of the protein as a whole, as is further borne out by the NMR data.

The temperature dependence of the extinction coefficients for native[2] and unfolded nitrated RNase made it difficult to extrapolate to an accurate value of the difference in amplitude between native and unfolded states at −15 °C. As a consequence, we chose to compare the extinction coefficients in cryosolvent at −15 °C by using Gdn·HCl to unfold the protein. The molar extinction coefficients determined in this way are shown in Table III. The calculated contributions to the observed extinction coefficients of the individual nitrotyrosines are also included. The value for nitro-Tyr-73 at pH* 6 is clearly anomalous, probably reflecting a significantly perturbed pK of nitro-Tyr-73 when Tyr-115 is nitrated, due to the H bond present in the unmodified protein.

Refolding Kinetics. Since the nitrotyrosyl absorbance band is well resolved from that of the remaining aromatic residues, the environment about specific tyrosine residues can be

[2] The temperature dependence of the extinction coefficients for nitrated native ribonuclease was very different from that of nitrated *N*-acetyl-L-tyrosine ethyl ester.

Table IV: Kinetics of Refolding of RNase at −15 °C, in 35% MeOH[a]

	pH* 3.0				pH* 6.0			
signal	k_I(Amp)[b] × 10^2	k_{II}(Amp) × 10^2	k_{III}(Amp) × 10^3	k_{IV}(Amp) × 10^4	k_I × 10^2	k_{II}(Amp) × 10^2	k_{III}(Amp) × 10^3	k_{IV}(Amp) × 10^4
ΔA_{286}	6.2 ± 0.9 (dec)	1.3 ± 0.4 (19)	1.7 ± 0.4 (19)	2.9 ± 1.0 (19)	5.4 ± 1.2	1.0 ± 0.2 (−8)	3.3 ± 0.9 (9)	7.3 ± 1.0 (8)
115-NO_2	2.6 ± 0.6	0.88 ± 0.2 (37)	–	–	8.5 ± 1.0	1.6 ± 0.3 (26)	–	–
115,76-NO_2	2.3 ± 1.0	1.4 ± 0.2 (37)	0.82 ± 0.07 (9)	–	11.0 ± 2.0	1.6 ± 0.4 (12)	2.1 ± 0.6 (8)	–
76-NO_2	ND	1.8 ± 0.6 (40)	0.71 ± 0.06 (7)	–	ND	1.1 ± 0.1 (15)	1.8 ± 0.1 (10)	–
115,76,73-NO_2	3.0 ± 0.7	0.75 ± 0.1 (26)	1.3 ± 0.4 (18)	–	4.0 ± 2.0	0.7 ± 0.06 (13)	1.5 ± 0.5 (10)	–
73-NO_2	ND	–	1.8 ± 0.7 (41)	–				
115-NO_2/A_{286}	ND	ND	1.1	3.7	ND	ND	2.6	4.3
115,76-NO_2/A_{286}	ND	ND	2.3	3.5	ND	ND	2.6	4.3
115,76,73-NO_2/A_{286}	ND	ND	ND	6.0	ND	ND	ND	7.4

[a] The values in parentheses are the amplitudes expressed as a percentage of the total amplitude difference between U and N under the experimental conditions. The data for ΔA_{286} are shown for comparison (Biringer & Fink, 1988). [b] Rate constants are in units of s^{-1}, Amp = amplitude, ND means not determined, (–) means the reaction was not observed, 115-NO_2/A_{286} indicates refolding monitored at 286 nm, and the errors shown are the standard deviations.

monitored without interference from other tyrosines. The folding of nitrated ribonuclease A in aqueous solution has been previously reported (Garel, 1980; Garel & Baldwin, 1975); analysis of the sample indicated approximately 2.7 nitro-Tyr/protein; thus the preparation appeared to be predominantly the trinitro derivative (Garel & Baldwin, 1975). The change in absorbance of the nitrotyrosine residues was found to be due to a shift in the pK upon burial of the nitrotyrosine during folding. For this derivative the reported kinetics were biphasic, and the faster of the two phases resembled that observed by absorbance in the kinetics of refolding of unmodified RNase A, in terms of the rate and activation enthalpy dependence on Gdn·HCl concentration. For the slower phase the rate and activation enthalpy were independent of the Gdn·HCl concentration. Since such independence had been shown to be associated with proline isomerization, it was concluded that the slow step was limited by this process.

In the present study the kinetics of refolding were measured under the following final conditions: in 35% (v/v) methanol, at −15.2 ± 0.2 °C, and at both pH* 3.0 and pH* 6.0. The refolding kinetics of the mononitro derivative are shown in Figures 6A and 7A for folding at pH* 3.0 and 6.0, respectively. The results provide information on the rate at which the environment about tyrosine-115 becomes native-like. At both values of pH the kinetics were found to be biphasic. The rates and amplitudes are given in Table IV and represent an average of five experiments. The constraints imposed by the length of time (30–50 s) required for complete thermal equilibration at the beginning of the refolding experiment precluded precise measurement of the amplitudes of the fastest observed phase. In all cases data were collected for longer time periods than those shown in the figures. Our criterion for completion of the reaction was a stable base line for at least 1000–2000 s.

Similar kinetics were observed when the refolding was done with protein that had been unfolded with 5 M Gdn·HCl (Table V). However, the effective "dead time" of the system was often considerably longer when 5 M Gdn·HCl was added (as long as 100 s in some instances), leading to difficulties in monitoring the early stages of the refolding progress and compounding the difficulties in measuring the amplitudes of the faster phases. The problems arise from the large difference in refractive index and viscosity of the guanidinium solution compared to those of the cryosolvent. Some caveats associated with the use of thermally unfolded protein in refolding kinetics experiments at subzero temperatures are discussed subsequently (Biringer & Fink, 1988). However, the fact that both thermally unfolded and Gdn·HCl-unfolded samples gave similar results indicates that relatively little additional refolding occurred during the time of mixing due to the initially high temperature for the thermally unfolded material.

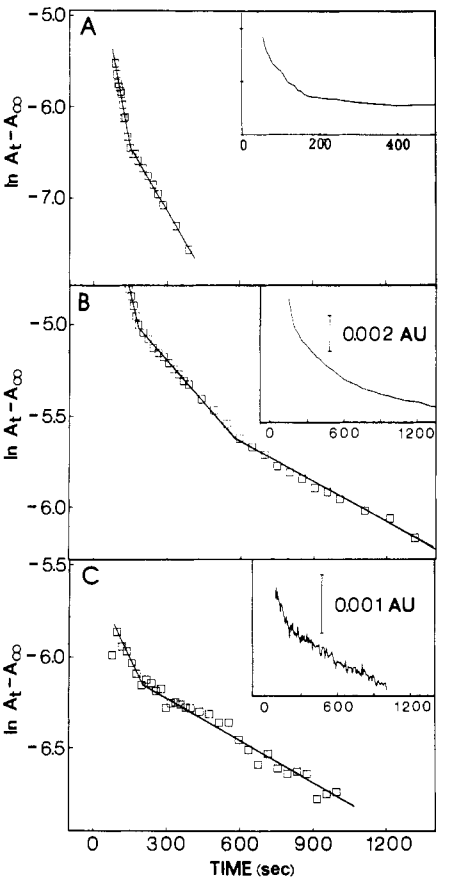

FIGURE 6: Time-dependent changes in the refolding of nitrated ribonucleases in 35% methanol, pH* 3.0, at −15 °C. Semilog plots are given with a sampling of data points to show the biphasic nature of the data. The insets show the absorbance traces. (A) $C^{\epsilon 115\text{-}NO_2}$-RNase, 34.5 μM; (B) $C^{\epsilon 115,76\text{-}NO_2}$-RNase, 24.1 μM; (C) ϵ-nitro-Tyr-76 calculated by difference (see text).

The data indicate that a significant portion of the protein (63% at pH* 3 and 74% at pH* 6) attains a native-like environment about Tyr-115 within, or prior to and within, the first observed step (k_I).[3] The remainder becomes native-like

[3] Rate constants from *observed* transients will be denoted by roman numeral subscripts, whereas those from model schemes will be indicated by arabic subscripts.

Table V: Comparison of Kinetics of Refolding of Guanidine Hydrochloride Unfolded and Thermally Unfolded Ribonuclease A at −15 °C, in 35% Methanol

sample[a]	signal[b]	unfolding[c]	k_I	Amp_I[d]	k_{II}	Amp_{II}
RNase, pH* 3	F_{305}	Gdn·HCl	1.3×10^{-3}	22	1.4×10^{-4}	9
RNase, pH* 3	F_{305}	thermal	1.3×10^{-3}	17	3.0×10^{-4}	7
RNase, pH* 6	F_{305}	Gdn·HCl	1.6×10^{-3}	21	3.9×10^{-4}	10
RNase, pH* 6	F_{305}	thermal	1.7×10^{-3}	19	3.1×10^{-4}	5
76,115-dinitro-Tyr, pH* 3	A_{300}	Gdn·HCl	1.7×10^{-2}	ND	1.4×10^{-3}	17
76,115-dinitro-Tyr, pH* 3	A_{300}	thermal	1.4×10^{-2}	37	8.2×10^{-4}	9

[a] RNase represents unmodified protein. [b] F_{305} corresponds to experiments in which the tyrosine fluorescence was monitored at 305 nm [see also Biringer and Fink (1988)]. [c] Unfolding was done either by 5 M Gdn·HCl or thermally, as described in the text. [d] The amplitudes are expressed as a percentage of the total amplitude difference between U and N under the experimental conditions. Rate constants are in units of s^{-1}. ND means not determined.

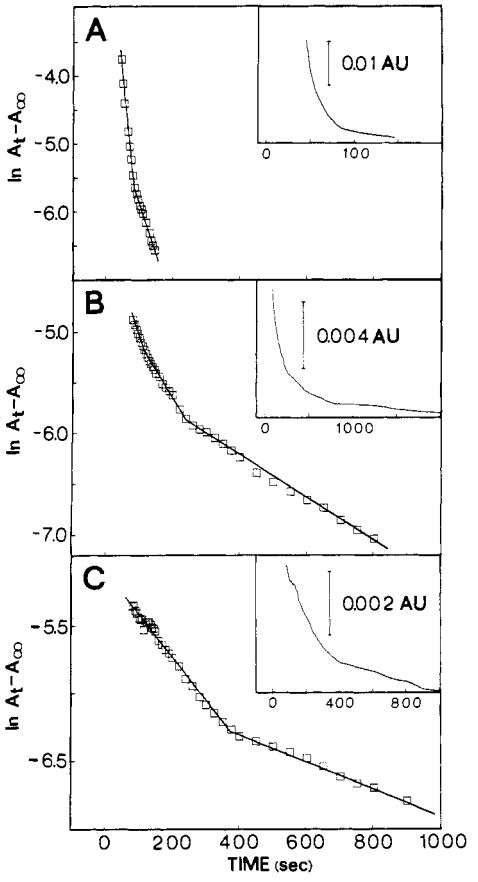

FIGURE 7: Time-dependent changes in the refolding of nitrated ribonucleases in 35% methanol, pH* 6.0, at −15 °C. Semilog plots are given with a sampling of data points to show the multiphasic nature of the data. The insets show the absorbance traces. (A) $C^{\epsilon 115\text{-}NO_2}$-RNase, 41.0 μM; (B) $C^{\epsilon 115,76\text{-}NO_2}$-RNase, 41.0 μM; (C) ϵ-nitro-Tyr-76 calculated by difference (see text).

in this region within 600 s at pH* 3 and 200 s at pH* 6. By contrast, full recovery of the native state and catalytic activity requires 12×10^3 s at pH* (Biringer & Fink, 1988; Biringer et al., 1988).

The dinitro derivative showed triphasic kinetics at both pH values (Figures 6B and 7B). The rate constants are given in Table IV and represent an average of six experiments for pH* 3.0 and eight for those at pH* 6.0.

The kinetics for refolding as monitored by nitro-Tyr-76 were obtained by subtracting the absorbance vs time plots of an average of three mononitro refolding experiments from the corresponding plots of individual dinitro-RNase refolding experiments. Prior to subtraction, the dinitrotyrosine data were multiplied by an appropriate factor to account for any differences in the protein concentration between the two sets of experiments. The resulting kinetic traces are shown in Figures 6C and 7C. At each pH* the folding appears biphasic (the fast phase observed in the original experiments was lost in the noise produced by the subtraction). The results were analyzed separately and are given in Table IV as an average of three such subtractions. The data in the figures are corrected to the concentrations used in the refolding experiments of the dinitro derivative. The theoretical maximum amplitude was assumed to be the difference between those expected for the mononitro and dinitro derivatives at the same concentrations. The rate constants are similar to those found for the dinitro derivative. The amplitudes of the slowest phase were unaffected by the subtraction as expected. The amplitudes indicate that 53% of the native signal for Tyr-76 returned in the fastest (k_I) phase, or a preceding step, at pH* 3 and 75% returned at pH* 6.

At both pH* 3 and 6 the trinitro derivative showed similar triphasic kinetics to those seen with the dinitro derivative. The rate constants are given in Table IV. A similar subtraction procedure to that described above for nitro-Tyr-76 was used to obtain the contribution of nitro-Tyr-73. A single slow phase (k_{III}) (Table IV) was found. The perturbation of the extinction coefficient for nitro-Tyr-73 at pH* 6 (see Table III) prevented accurate determination of the kinetic parameters at pH* 6. Extrapolation of the rate of refolding in aqueous solution for the nitrated RNase of Garel (1980) to −15 °C gives rate constants of 6.7×10^{-3} and 2.3×10^{-5} s^{-1} (pH 6.5). It is interesting to note that one of the transients we observe with the trinitro derivative, k_{II}, has a rate of 6.5×10^{-3} s^{-1} at −15 °C, pH* 6.0. No evidence of the slower phase observed by Garel (1980) in aqueous solution was noted in the present study.

Modification of a single amino acid residue may produce substantial change in the overall structure of a protein. Even a minor change could alter the pathway of folding. The NMR spectra, catalytic activities, and the midpoints of the unfolding transitions of the nitrated derivatives clearly show that in this case the modification (nitration) does little to alter the structure of the native protein. In order to determine if any minor structural changes would alter the folding path, the refolding of the nitrated derivatives was repeated with monitoring of the reaction by absorbance at 286 nm. At this wavelength both nitrated and unmodified tyrosines can be followed. If the pathway is unaltered, kinetics similar to those of unmodified RNase folding should be observed. The folding of each derivative bagan with a large decrease in absorbance corresponding to the burial of the nitrotyrosines, which masked the fastest two processes observed by ΔA_{286} in unmodified protein (Biringer & Fink, 1988). The rate constants obtained from the experiments are given in Table IV. The similarity in the observed rates for both RNase A and the derivatives suggests that the pathways of folding are not significantly perturbed by nitration of these three tyrosines. Since the slowest transient observed by ΔA_{286}, which arises from changes in the environment about Tyr residues, is still observed when

tyrosines-73, -76, and -115 are nitrated, we assume that the source of the signals is one or more of the other three tyrosines, probably Tyr-92 (Biringer & Fink, 1988).

Folding Pathway. Two immediate conclusions may be drawn from the refolding kinetics results: (1) The environment about Tyr-115 becomes native-like faster than that about Tyr-73 and Tyr-76 (Table IV, Figures 6 and 7). (2) The full native state is formed even more slowly than Tyr-73 and Tyr-76 attain their native environments (Table IV) (Biringer & Fink, 1988; Biringer et al., 1988). *Therefore, different regions of the molecule refold at different rates, implying a sequential folding pathway in which partially folded intermediates exist.*

At pH* 3 the fastest observed phase (k_I) for both nitro-Tyr-115 and -76 (as revealed by the dinitro derivative) has the same rate. Given the large experimental error for this fastest phase, it is likely that the same holds at pH* 6. Therefore, it appears that both probes are monitoring the same process. For pH* 3 the amplitude data from the slower phases indicates that these transients correspond to 30–35% of the expected change between slow-refolding unfolded material and the native site. For nitro-Tyr-115 the amplitude of the slower phase (k_{II}) decreases from 45% at pH* 3 to 26% at pH* 6. This suggests that at pH*3 two processes had rates equivalent to k_{II} and that at pH* 6 one of these processes become faster, accounting for the observed loss of 20% of the signal.

Data from a number of other types of experiments, including double-jump unfolding assays, NMR, fluorescence changes, inhibitor binding, and catalytic activity (Biringer & Fink, 1982b, 1988; Biringer et al., 1988), indicate that refolding of slow-folding material, under these experimental conditions, occurs via two parallel pathways. The minor pathway involves approximately 30% of the total unfolded protein; the major path is taken by 50%. The amplitude for the slower transient (k_{II}) for nitro-Tyr-115 at pH* 6 is 26% of the total. We thus assign this phase to the minor pathway. Similarly, the two slowest transients for nitro-Tyr-76 at pH* 6 have a combined amplitude of 25% and can be associated with the minor path. This assignment is also consistent with Tyr-76 being a major source of fluorescence change associated with folding (Krebs et al., 1985). The 25% in amplitude lost in the step with rate k_{II} for the mono- and dinitro-Tyr derivatives in going from pH* 3 to pH* 6 is ascribed to a process on the major slow-folding pathway with rate k_{II} at pH* 3 which becomes much faster at pH* 6. Since only 25% of the signal is associated with this step, k_2, the implication is that the intermediate I_1 that decays in this process must posses partial native-like environment about Tyr-76 and -115.

The fastest observed process, with rate k_I, is attributed to the step with rate k_1 in Scheme I. The observed transients, k_{II} and k_{III} for nitro-Tyr-76 and k_{II} for nitro-Tyr-115, are associated with steps k'_2 and k'_3 in the minor pathway, as discussed above. On the basis of the amplitude of the slower phase (k_{II}) for the nitro-Tyr-115 derivative at pH* 6 intermediate I'_1 must have a native-like environment around Tyr-115 but only a partial native-like environment about Tyr-76 (and presumably Tyr-73). I'_2 has a native-like environment about both Tyr-76 and Tyr-115 but is not fully native, on the basis of other probes.

Scheme I

$$U_F \rightarrow N \qquad (20\%)$$

$$U_S^{II} \xrightarrow{k_1} I_1 \xrightarrow{k_2} N \qquad (50\%)$$

$$U_S^{I} \xrightarrow{k'_1} I'_1 \xrightarrow{k'_2} I'_2 \xrightarrow{k'_3} N \qquad (30\%)$$

The data for nitro-Tyr-73 indicate that the environment about Tyr-73 is native-like prior to the slowest transients observed by other probes (Biringer & Fink, 1988; Biringer et al., 1988). The observed transient for nitro-Tyr-73 at pH*3, k_{III}, can be assigned either to the minor slow-refolding pathway, that is, formation of I'_2, in which case the rather large amplitude is attributed to specific effects on the value of the extinction coefficient, or to the major slow-folding pathway, in which case it would imply an additional intermediate between I_1 and N in Scheme I. On the basis of other, related data (Biringer & Fink, 1988), we favor the former interpretation.

The model of Scheme I is combined with data from measurements of refolding using other probes in a following paper (Biringer & Fink, 1988). Scheme I is the simplest model consistent with the results from the nitrated RNase derivatives. The present investigation demonstrates the great potential for using environment-sensitive probes located throughout the molecule to map out the pathway of protein folding.

Registry No. RNase, 9001-99-4.

References

Beaven, G. H., & Gratzer, W. B. (1968) *Biochim. Biophys. Acta 168*, 456–462.

Bevington, P. R. (1969) *Data Reduction and Error Analysis for the Physical Sciences*, pp 232–242, McGraw-Hill, New York.

Biringer, R. G., & Fink, A. L. (1982a) *J. Mol. Biol. 160*, 87–116.

Biringer, R. G., & Fink, A. L. (1982b) *Biochemistry 21*, 4748–4755.

Biringer, R. G., & Fink, A. L. (1988) *Biochemistry* (third of three papers in this issue).

Biringer, R. G., Austin, C. M., & Fink, A. L. (1988) *Biochemistry* (second of three papers in this issue).

Campbell, R. L., & Petsko, G. A. (1987) *Biochemistry 26*, 8579–8584.

Fink, A. L., & Painter, B. (1987) *Biochemistry 26*, 1665–1671.

Fink, A. L., Kar, D., & Kotin, R. (1987) *Biochemistry 26*, 8571–8579.

Garel, J. R. (1980) *Biochem. Biophys. Res. Commun. 91*, 1339–1345.

Garel, L., & Baldwin, R. L. (1975) *J. Mol. Biol. 94*, 621–632.

Goto, K., Takahashi, N., & Murachi, T. (1971) *J. Biochem. (Tokyo) 70*, 157–164.

Kim, P. S., & Baldwin, R. L. (1982) *Annu. Rev. Biochem. 51*, 459–489.

Krebs, H., Schmid, F. X., & Jaenicke, R. (1985) *Biochemistry 24*, 3846–3852.

Lenstra, J. A., Bolscher, B. G. J. M., Stob, S., Beintema, J. J., & Kaptein, R. (1979) *Eur. J. Biochem. 98*, 385–397.

Mui, P. W., Konishi, Y., & Scheraga, H. A. (1985) *Biochemistry 24*, 4481–4489.

Nall, B. T., & Baldwin, R. L. (1977) *Biochemistry 16*, 3572–3576.

Nall, B. T., Garel, J., & Baldwin, R. L. (1978) *J. Mol. Biol. 118*, 317–330.

Petersen, S. (1981) *Sci. News (Washington, D.C.) 120*, 317.

Schmid, F. X. (1981) *Eur. J. Biochem. 114*, 105–109.

Schmid, F. X. (1983) *Biochemistry 22*, 4690–4696.

Schmid, F. X., & Baldwin, R. L. (1979) *J. Mol. Biol. 135*, 199–215.

Schmid, F. X., & Blascheck, H. A. (1981) *Eur. J. Biochem. 114*, 111–117.

Schmid, F. X., Grafl, R., Wrba, A., & Beintema, J. J. (1986)

Proc. Natl. Acad. Sci. U.S.A. 83, 872-876.
Seagle, R. L., & Cowgill, R. W. (1976) *Biochim. Biophys. Acta 439*, 470-478.
Van Der Zee, R., Duisterwinkel, F. J., & Welling, G. W. (1977) *Eur. J. Biochem. 77*, 125-131.
Vincent, J. P., Lazdunski, M., & Delaage, M. (1970) *Eur. J. Biochem. 12*, 250-257.
Williams, J., & Lowe, J. M. (1971) *Biochem. J. 121*, 203-209.

Intermediates in the Refolding of Ribonuclease at Subzero Temperatures. 2. Monitoring by Inhibitor Binding and Catalytic Activity†

Roger G. Biringer,‡ Craig M. Austin, and Anthony L. Fink*
Department of Chemistry, The University of California, Santa Cruz, California 95064
Received September 29, 1986; Revised Manuscript Received July 13, 1987

ABSTRACT: The kinetics of refolding of ribonuclease A were monitored by the return of catalytic activity and inhibitor binding at −15 °C in 35% methanol cryosolvent at pH* 3.0 and 6.0. Catalytic activity was measured with cytidine 2′,3′-cyclic monophosphate as substrate; inhibitor binding was determined with the competitive inhibitor cytidine 2′-monophosphate. Biphasic kinetics were observed at pH* 3.0 for both return of catalytic activity and inhibitor binding. At pH* 6.0 the rate of return of catalytic activity was monophasic, whereas that of inhibitor binding was biphasic. For both inhibitor binding and catalytic activity one of the observed rates was pH-dependent. Full return of catalytic activity was obtained at the completion of the refolding process. The observations are interpreted in terms of two parallel pathways of refolding for slow-refolding ribonuclease, with several native-like, partially folded intermediate states on the minor slow-refolding pathway. Of particular note is the presence of at least one such species that has inhibitor-binding capacity but not catalytic activity. This may be rationalized in terms of the known native structure. In addition, an intermediate is postulated which has the incorrect Pro-93 conformation and only partial catalytic activity (42% of the native). The slowest observed transient is attributed to the isomerization of this proline residue and return of full catalytic activity.

This paper is the second in a series in which the folding of ribonuclease A (RNase)[1] was studied in aqueous methanol cryosolvents and at subzero temperatures. These conditions were used in order to facilitate the detection of partially folded intermediate states in the folding process. Previous investigations have shown that the native state of RNase in 35% methanol is essentially the same as that in aqueous solution (Biringer & Fink, 1982a) and that the refolding process is multiphasic (Biringer & Fink, 1982b, 1988a,b). In the present research we have used the ability of the folded enzyme to bind competitive inhibitors and to catalyze the hydrolysis of substrate as a means of measuring the rate at which the native protein is formed. We assume that only a native-like state will possess a competent catalytic apparatus, although inhibitor binding could occur with only a partially formed active site.

Experimental Procedures

Materials

Ribonuclease A was purified as described previously (Biringer & Fink, 1982a, 1988a,b). 2′,3′-CMP and 2′-CMP were purchased from P-L Biochemicals and used without further purification. Methanol was HPLC grade, and buffer materials were AR grade. Cryosolvents were prepared as described previously (Biringer & Fink, 1988a).

Methods

Inhibitor Binding. Refolding kinetics were measured by using the binding of 2′-CMP to monitor the formation of the inhibitor binding site. The stoichiometry of the binding has been determined to be 1:1 in aqueous solution (Schmid & Blascheck, 1981) and is presumed to be the same in cryosolvent. The protein was unfolded by heating a stock solution (0.5 mM) in 35% methanol, pH* 3.0, at 70 °C for 10 min, which has been shown to fully unfold the protein as judged by proton NMR (Biringer & Fink, 1982a). The unfolded enzyme was injected into 0.8 mL of solution containing 100 μM 2′-CMP in 35% methanol (0.033 M sodium formate, pH* 3.0, or 0.033 M sodium acetate, pH* 6.0) at −15 °C. The reaction was monitored at 254 nm for the pH* 6.0 experiments and at 271.5 nm for the pH* 3.0 experiments. The isosbestic point for the enzyme folding when followed by UV absorbance is 254 nm and is independent of pH. At pH* 6.0 the binding reaction can be monitored without interference from the folding. At pH* 3.0 the *binding* reaction also exhibits an isosbestic point at 254 nm. At 271.5 nm a minimal change in absorbance due to protein (i.e., tyrosine burial) is observed whereas a large change due to 2′-CMP binding can be seen. The small contribution of the absorbance change due to protein

† This research was supported by grants from the National Science Foundation.
‡ Present address: Department of Chemistry, San Jose State University, San Jose, CA 95192.

[1] Abbreviations: RNase, ribonuclease A; 2′-CMP, cytidine 2′-monophosphate; 2′,3′-CMP, cytidine 2′,3′-cyclic phosphate; NMR, nuclear magnetic resonance; N, native state; U, unfolded state; pH*, apparent pH of aqueous–organic cryosolvent, as determined with glass electrode/pH meter; HPLC, high-performance liquid chromatography; AR, analytical reagent.

0006-2960/88/0427-0311$01.50/0